Geosci. Instrum. Method. Data Syst. Discuss., doi:10.5194/gi-2016-22, 2016
Manuscript under review for journal Geosci. Instrum. Method. Data Syst.
Published: 23 August 2016

Geoscientific Instrumentation Methods and Data Systems Discussions
Open Access
EGU

CONTINUOUS WAVELET TRANSFORM AND EULER DECONVOLUTION METHOD AND THEIR APPLICATION TO MAGNETIC FIELD DATA OF JHARIA COAL FIELD, INDIA

Arvind Singh and Upendra Kumar Singh
Department of Applied Geophysics, Indian School of Mines, Dhanbad, India-826004

1. Abstract

This paper deals the application of Continuous Wavelet Transform (CWT) and Euler deconvolution methods to estimate the source depth using magnetic anomalies. These methods are utilised mainly to focus on the fundamental issue for mapping the major coal seam and locating magnetic lineaments. These methods are tested and demonstrated on synthetic data and finally applied on field data from Jharia coal field. Prepared magnetic anomaly map that reflects clear tectonics control and nature of the underlying basement, demarcation of the basin, geological faults by steep gradients of magnetic anomaly. Analysis suggests that the CWT have a great utility in the magnetic data interpretation and the correlation between magnetic anomalies and geological features such as faults/joints and intrusive bodies over the basin. The CWT provides the consistent and reliable depth of the underlying basement with the results of Euler deconvolution and Tilt-depth methods without any priory information that is correlated well with borehole samples (Raja Rao, 1987).

One of the fundamental issues is to detect differences in susceptibility and density between rocks that contain ore deposits or hydrocarbons or coal. These differences are reflected in the gravity and magnetic anomalies and also delineation of structural features, which are interpreted using several techniques (Blakely and Simpson, 1986). One of the most important objective in the interpretation of potential field data is to improve the resolution of underlying source, delineating lateral change in magnetic susceptibilities that provides information not only on lithological changes but also on structural trends.

Especially, mapping the edges of causative bodies is fundamental to the application of potential field data to geological mapping. The edge detection techniques are used to distinguish between different sizes and different depths of the geological discontinuities (Cooper and Cowan 2006, 2008; Perez et al. 2005; Ardestani 2010; Hsu et al. 1996, 2002; Holschneider et al., 2003). The derivatives of magnetic data are used to enhance the edges of anomalies and improve significantly the visibility of such features.

Sedimentary layer dominates the gravity and magnetic signature over Jharia Coal field (Verma et al., 1973, 1976, 1979). Thus the difference between the depths estimated using Euler deconvolution method (EDM) (Thompson 1982; Reid et al. 1990) and Tilt Depth Method (TDM) technique (Salem et al., 2007; Cooper 2004, 2011) may help to detect the thickness of the coalbed. Wavelet transform and Euler deconvolution method has been theoretically demonstrated on magnetic data. These methods provide source parameters such as the location, depth, geometry of geological bodies and interfaces in an easy and effective way. However, it may be more difficult to characterize the source properties in cases of extended sources (Sailhac et al., 2009).

These methods executed over Jharia coal field, Dhanbad, India. This area forms an east west trending belt of Gondwana basin of Damodar valley at the north eastern part of India. This study region is mostly coal rich area of Gondwana basin. Analysis on Jharia coal field suggests that the magnetic anomalies provide encouraging results which are well correlated with available gravity data and some borehole informations.

2. Geology of Jharia coal field

Geology of the Jharia coal basin is shown in Fig. 1. The basin has been formed because of crustal subsidence during Gondwana periods (Fox, 1930). The coal field have extension along the east west direction in Gondwana basin of Damodar valley at the north eastern part of the India. Gondwana basin is surrounded by crystalline gneisses of several categories from all the directions. Sedimentary strata have the inclination away from the gneiss contact in this region. The sedimentary strata include the rocks which belong to Talchir, Raniganj series, Barren-measures formation and Barakar series (Verma et al, 1979). Raniganj series, Barakar series and Talchir series including barren measures formation covers area about 58 km^2, 218 km^2 and 181 km^2 respectively. Various formations are shown in the Figure 1.

Geosci. Instrum. Method. Data Syst. Discuss., doi:10.5194/gi-2016-22, 2016
Manuscript under review for journal Geosci. Instrum. Method. Data Syst.
Published: 23 August 2016

Geoscientific Instrumentation Methods and Data Systems Discussions
Open Access

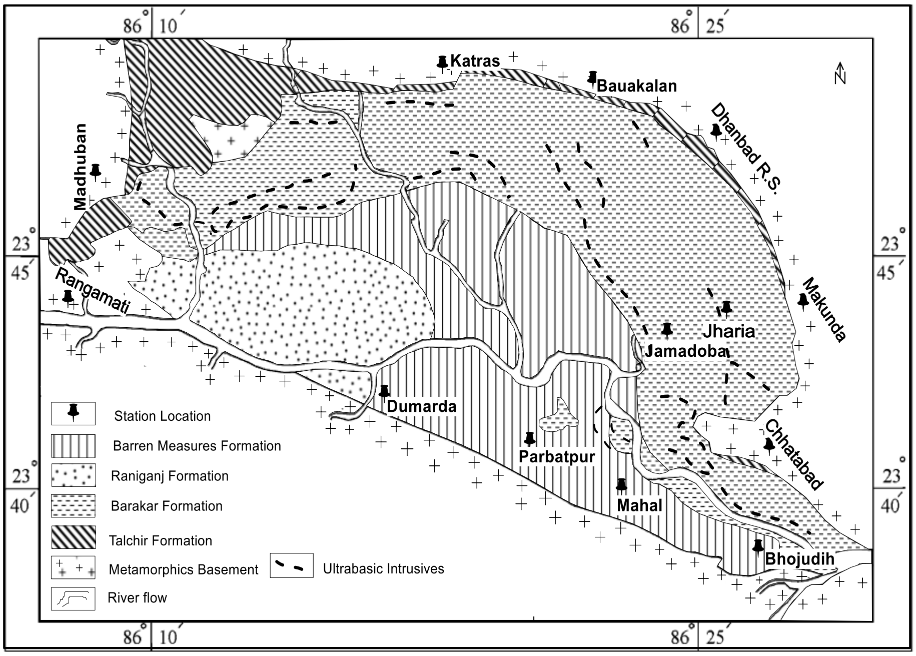

Figure 1: Geological map of Jharia coal field and surrounding regions, (after Verma et al, 1979)

Talchir and Barakar formation rest over northern margin and having dip towards the southern margin. Barakar Series covers northern half of this coal field. Barakar series produces the best quality coal in India. An elliptical outline is formed by Raniganj formation in south western region of the coal field. Geology of the Jharia coal field has been divided into many blocks like Parbatpur block, Mahuda block, Jarma and Monidih block etc. There are many faults exist over Jharia coal field. A normal tensional fault exists over the southern boundary. In the south western part of the basin Damodar river (Fig. 1) flows very close to the southern boundary fault (Verma et al, 1973, 1979, Verma and Ghosh, 1974).

Geosci. Instrum. Method. Data Syst. Discuss., doi:10.5194/gi-2016-22, 2016
Manuscript under review for journal Geosci. Instrum. Method. Data Syst.
Published: 23 August 2016

Geoscientific Instrumentation Methods and Data Systems
Discussions
Open Access

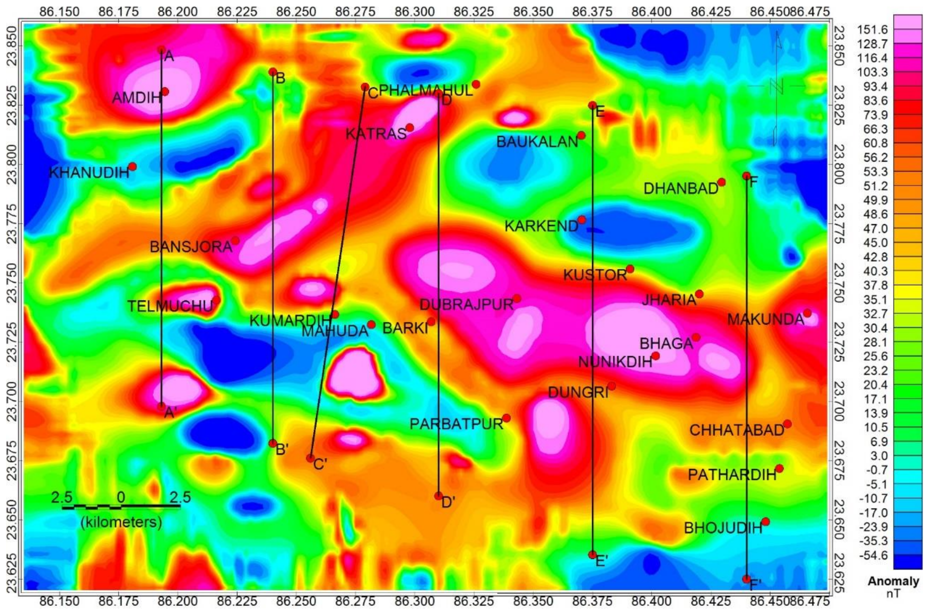

Figure 2: Total magnetic field anomaly (nT) map and location of the profiles over Jharia coal field and surrounding regions (after Verma et al., 1979).

The Magnetic data has been obtained from Verma et al (1979) to study the region. After, all necessary corrections, we prepared the total magnetic anomaly map with the help of magnetic data of this province as shown in Fig. 2. The map shows very sharp and irregular pattern outcrops, while over the basin the variations of magnetic anomalies are smooth and the northern part of the basin the magnetic anomalies over this region suggest that basin is identical to a curve. In the southern part, the anomalies are fairly parallel to the southern boundary fault and there is no clear indication of the trend of the anomalies in the south eastern part, which is probably due to its irregular faulting associated with Pathardih horst. Obviously the anomaly map reflects the sediments have been highly folded and faulted and coal seams have been highly deformed. A noticeable part of the magnetic anomaly is the presences of major anomalous source, which are ascribed to some features within the Precambrian basement underlying sediments.

Geosci. Instrum. Method. Data Syst. Discuss., doi:10.5194/gi-2016-22, 2016
Manuscript under review for journal Geosci. Instrum. Method. Data Syst.
Published: 23 August 2016

3. Methodologies

3(a). Continuous Wavelet Transform

The continuous wavelet transform is the conversion of any signal into matrix made of sum scaler products in Fourier space. Wavelet Transform method for potential field has been established by Moreau et al. (1997, 1999). This method previously used for homogeneous, isolated and extended potential field sources (Sailhac et al., 2009). Chamoli (2006); Cooper (2006); Goyal and Tiwari (2014); Singh and Singh (2015) used wavelet transform method on various synthetic as well as on field data. Method allows Poisson group of wavelets as a mother wavelet in order to interpret the potential field data. To analyse the signal by mother wavelet, a wavelet domain signal is decomposed into the orthogonal wavelets of finite duration. The CWT coefficient W_t of a measured potential t(x) is defined as the convolution product.

$$W[\psi,t](p,o)=\int_{R^n}\frac{1}{o^n}t(x)\psi\left[\frac{p-x}{o}\right]dx \tag{1}$$

$$W[\psi,t](p,o)=(D_o\psi*t)(p) \tag{2}$$

where ψ ($x \in R^n$) is the wavelet to be analysed; x denotes the abscissa along the particular profile line; t(x) indicates the potential field (gravity or magnetic anomaly); ($o \in R^+$) and p are the dilation and position parameter respectively. Dilation parameter allows analysing wavelet to act as a band pass filter. Dilation operator D_o can be termed as

$$D_o\psi(x)=\frac{1}{o^n}\psi\left(\frac{x}{o}\right) \tag{3}$$

dilation D_o fulfils two properties given below

(i) $$W[\psi,D_\lambda t](p,o)=\frac{1}{\lambda^n}W[\psi,t]\left(\frac{p}{\lambda},\frac{o}{\lambda}\right) \tag{4}$$

above equation states that the main mathematical asset of wavelet transform (i.e. covariance of wavelet transforms with respect to the dilation) and

(ii) Homogeneous function t of degree $\sigma \in R$ can be define as

$$t(\lambda,x)=\lambda^\sigma t(x)\forall\lambda>0 \tag{5}$$

after correlation equations (4) and (5) result homogeneous function (i.e. by recalling σ=-n and σ=0, respectively)

$$(\lambda p, \lambda o)W[\psi,t] = \lambda^{\sigma} W[\psi,t](p,o) \qquad (6)$$

Equation (6) represents that wavelet transform of a homogeneous function is analogous to dilation and scale of any function $W(\psi,t)(p,o = consant)$ of the wavelet transform. Moreau et al., (1999) suggest that the combinations of straight lines creates a cone like outline at the location where $\left(\frac{\partial^m}{\partial p^m}\right) W(\psi,t)(p,o) = 0$ and apex of the outline is the centre of homogeneity of the analysed function. The outlines in the Fig. (3) fulfils the condition $\left(\frac{\partial^m}{\partial p^m}\right) W(\psi,t)(p,o) = 0$ are known as edges of wavelet transform or modulus maxima lines.

Potential field signal analysed by CWT allows for estimation of depth and homogeneous distribution order of the source generating the analysed signal. Source depth is calculated through the intersection of the converging extrema lines (Fig. 3). In addition to this, Moreau et al. (1997, 1999) established the Poisson semi group kernel $K_o(x)$, which allows to carry on the harmonic field $t(x,z)$ from level z to the level z+o, and expressed as upward continuation (Bhattacharyya, 1972).

$$P_o(x) = \frac{o}{\pi}\left(\frac{1}{o^2 + x^2}\right) \qquad (7)$$

For wavelet analysis, let us consider a local homogeneous source $x = 0$ having depth $z = z_{\alpha}$, of a potential field $t(x, z = 0)$. Moreau (1999) stated that the wavelet coefficients of positions and dilations lie in the upper half plane follow a twice scaling rule with two exponent parameters. Moreau (1997) explained the relationship between wavelet coefficients at two altitudes and for any wavelets of homogeneous sources as

$$W[\psi,t](p,o) = \left(\frac{o}{o'}\right)^{\gamma} \left(\frac{o'+z_{\alpha}}{o+z_{\alpha}}\right)^{\beta} W\left(p\frac{o'+z_{\alpha}}{o+z_{\alpha}}, o'\right) \qquad (8)$$

Where β= γ-σ-2 indicates the holder exponent, o and o′ denote different altitudes while Z_{α} signifies the depth of the causative source. Equations (6) and (8) have additional value in dilation and scaling in right hand side causes geometrical conversion of equation

(8). Due to geometrical conversion the cone like outline joins at source depth because of the negative dilation $o=z_\alpha$. Therefore, Poisson group of wavelets used on potential field demonstrate modest assets and can be applied to find the causative source without any prior information. CWT gives an idea to describe edges of the extended body. Also, it offers quick and consistent results about extended and isolated source depth with location. Wavelet analysis plays key role in depth estimation of potential field. When order of γ increases then obtained source depth appears shallower. For $\gamma=1$, outlines of the cone have the point of intersection at barycentre of the prismatic source. CWT can resolve the noisy and non-stationary dataset very well (Moreau; 1997, 1999) and magnetic data can also be analysed without any reduction to pole.

3(b). Euler deconvolution Method

Euler deconvolution was first developed for interpretation of magnetic profile data by Thompson (1982) and later Reid et al. (1990) extended its approach to gridded magnetic data. Reid et al. (1990) developed the special case for magnetic field of a contact of finite depth extent and coined the term "Euler deconvolution". Klingele et al. (1991) and Zhang et al. (2000) used it over gravity vertical gradient and tenser gravity gradient respectively. Moreover, it has been generalised by Mushayandebvu et al. (2001, 2004) and Rawat (1996) executed further to investigate the wider range of source nature. Since then, it has been adapted and improved to interpret the gravity data by Keating (1998). Euler Deconvolution Method (EDM) makes rapid depth estimations from magnetic and gravity data in grid form using Euler´s homogeneity relation (Thompson, 1982; Reid et al., 1990; Barbosa et al., 1999). Euler deconvolution is insensitive to magnetic inclination, declination and remanent magnetisation and is very suitable for 3D analyses (Keating, 1998; Mushayandebvu et al., 2004; Stavrev and Reid, 2007; Melo et al., 2013, Silva, et al., 2001).

The global acceptance of Euler deconvolution is mainly due to its simplicity of implementation and use, making it the tool of choice for a quick and reliable tool of interpretation for potential field data (FitzGerald et al., 2004; Gerovska and Arauzo Bravo, 2003) and to find the source information in terms of depth and geological structure. Euler deconvolution uses three orthogonal gradients of any potential quantity as well as the potential quantity itself to determine depths and locations of a source body. This method primarily responds to the gradients in the data and effectively traces the edge and defines the depth of the source body. Reid et al., (1990) and Thompson (1982) defined the 3-D Euler equation as.

$$(x-x_0)\frac{dF}{dx}+(y-y_0)\frac{dF}{dy}+(z-z_0)\frac{dF}{dz}+NF=0 \qquad (9)$$

Where (x_0, y_0, z_0) is the location of magnetic source whose total magnetic field (F) is observed at (x, y, z). The values dF/dx, dF/dy and dF/dz are the measured magnetic gradients along the x, y, and z directions. Euler deconvolution adds an extra dimension to the interpretation. It estimates a set of (x, y, z) points that, ideally, fall inside the source of the anomaly. Euler deconvolution requires the x, y, and z derivatives of the data and a parameter called the structural index (SI) N (N is non-negative integer). SI defines the anomaly attenuation rate at the observation point and depends on the geometry of the source. The SI is an integer number that is related to the homogeneity of the potential field and varies for different fields and source types (Stavrev and Reid, 2007; Barbosa et al., 1999 and Melo et al., 2013). For example, in the case of total field magnetic anomaly data, a dike is represented by an SI of 1, whereas a sphere is represented by an SI of 3.

The source points that are calculated as solutions by EDM are positioned at the estimated edge of the susceptibility inhomogeneities. Thus, the EDM relies on the derivatives of the magnetic data, the resulting depth estimates relate mainly to the areas of basement heterogeneities identified as distinct sources of the field. The first vertical gradient of magnetic data is calculated by using the fast Fourier transform (FFT) method (Gunn, 1975). The vertical and horizontal derivatives of the first vertical gradient, essential for the calculation of Eq. (9), are also been calculated using the FFT method. The horizontal source locations from EDM solutions can be used for explanation of lithological and structural trends. A location in the map where these solutions tend to make cluster is considered to be the most probable location of the source.

Equation (9) can be explained in terms of least square to estimate the source coordinates and structure. Since the absolute value anomalous field (F) is barely identified so equation (9) cannot be used directly over the observed data. Moreover, according to Thompson, (1982) equation (9) does not explain the regional or background magnetic field due to adjacent source, so obtained solutions may be unreliable and may vary from their accurate location.

For 2-D model, estimation of total magnetic field (F) and its derivatives at all points of data value provide the linear equation with unknown coordinates (x_0, z_0), where x_0, z_0 represents location and depth of the magnetic source respectively.

Using Taylor series unidentified regional field (E) can be described as follows

$$E(x,y) = E_0 + x\frac{\partial E}{\partial x} + y\frac{\partial E}{\partial y} + K(2) \qquad (10)$$

Where E_0 and K(2) represent the constant background for definite window and other higher order values in Taylor series expansion. The resultant anomalous field (F) can now be specified as the difference between the observed magnetic field (O) and regional magnetic field (E).

$$F = O - E \qquad (11)$$

Now after revision modified Euler equation can be specified as

$$O \equiv (x - x_0)\frac{d(O-E)}{dx} + (y - y_0)\frac{d(O-E)}{dy} + (z - z_0)\frac{d(O-E)}{dz} + N(O-E) = 0 \qquad (12)$$

According to Thompson (1982), Silva et al. (2003) and Reid et al. (1990), Euler equation provides satisfactory results by considering the first order term in Taylor series expansion. Also, Euler equation converts nonlinear and is resolved linearly by supposing tentative values of the structural index (Stavrev, 1997). Higher order term of Taylor series expansion provides the solution when singular points are closely spaced to each other (e.g. in the case of the multiple fracture, sill etc.). In this case postulation of linear background discontinues and needs higher order terms of Taylor series expansion for reasonable result.

Dewangan et al. (2007); Gerovska, and Arauzo Bravo (2003) chose the second order terms of the Taylor series expansion and favour to procedure of rational calculation in which the infinite Taylor series expansion is estimated by two polynomials (one lies in numerator and other one in denominator). Kopal (1961) suggested that the maximum accuracy in rational calculation may be possible when the polynomials of numerator and

Geosci. Instrum. Method. Data Syst. Discuss., doi:10.5194/gi-2016-22, 2016
Manuscript under review for journal Geosci. Instrum. Method. Data Syst.
Published: 23 August 2016

Geoscientific Instrumentation Methods and Data Systems Discussions
Open Access

denominator holds the same power. The rational function is used to calculate the background, this function can be defined as

$$E(x,y)=\left(\frac{E_0+ax+by}{1+cy+dy}\right) \qquad (13)$$

Where, a, b, c, d and E_0 are the unknown parameter. Comparison of the value of equation (13) and equation (12) generates another nonlinear Euler equation which provides the source depth, location and structural index (Coleman and Li, 1996, Williams et al., 2003). All the variation on Euler deconvolution includes working through profile as well as gridded data set using moving window (each window position is a set of linear equation which generates the solution to locate the source in plan and depth). The advantage of this method is that source magnetization direction and its result are not affected by the presence of remanence (Ravat, 1996). Moreover, it can be further used as inversion algorithm and the design rules based on mathematical analysis are proposed by Reid et al. (2014) must be considered to analyse the potential field (gravity and magnetics).

4. Modelling and Inversion of Gravity and Magnetic data

It is difficult to separate two anomaly sources with conventional method when the spatial scales of the sources are similar. Therefore, in order to explore new sources, it is necessary to study the inversion method and technique of two layer interfaces for potential fields (gravity and magnetic). If the basement consists of both a density and a magnetic interface, significant tectonic information about the source depth can be revealed through joint gravity and magnetic inversion by including the information of magnetic basement, minimizing the inversion ambiguity, and enhancing the inversion reliability.

Joint gravity and magnetic inversion methods started by Bott and Ingles (1972) by using an equivalent layer approach to find the variation in magnetization and density ratio of sources at the latter stage of the last century. Moreover, Menichetti and Guillen (1983) used a generalized inversion method to define sources shape for the 2.5D case. Zeyen and Pous (1993) deliberate the joint inversion problem on the basis of a priori information such as density, susceptibility and remnant magnetization of buried source. Zhang et al. (1993) established a method to invert gravity and magnetic data of the same layer with density and magnetism and developed a general linear integral inversion method. Gallardo Delgado et al. (2003) extended the 3D approach to include a density variation with depth and the magnetization direction as unknown parameters. In order to determine the topography of an interface of constant density and magnetization contrast a damped least squares method was used by Pilkington (2006) for joint inversion of gravity and magnetic data.

Wu et al. (2007) proposed the concept of a joint gravity and magnetic inversion of a variable density interface which better matches with actual geologic conditions. Practically, it is difficult to describe the nature of the misfit function or cost function as it relates to the results and appraisal of geophysical inverse problem. Fernandez Martinez et al., (2012, 2013) described the uncertainty in linear and nonlinear least squares inverse problems and proposed new insights to understand uncertainty in inverse problem very effectively. Jiang Fan et al. (2008) proposed and explain the effectiveness of the method of joint gravity and magnetic inversion for two layer models by associating the thickness changes and position of the middle layer and anomaly.

5. Application of CWT to Synthetic Magnetic Anomaly

The synthetic examples demonstrate the application of the CWT technique on the magnetic anomaly due to isolated and extended homogeneous magnetic sources at the position at 300 m having depth about 20 m. First analysis (shown in Fig. 3) corresponds to the magnetic anomaly of a finite length vertical dipole. The wavelet coefficients of magnetic field due to vertical dipole computed with the help of wavelet is shown in this figure (for horizontal derivative γ=1) which shows a cone like structure. Wavelet transform of the potential field due to homogeneous source follows a geometrical property which allows an easy estimation of source depth and location. The examples demonstrated could correspond to the zero remanent magnetization with all magnetization being induced. To understand the behaviour of the modulus maxima of CWT over of the magnetic anomaly due to the anomalous sources, the CWT is presented for various field examples. The converging point of ridges gives depth and location of the vertical dipole.

Geosci. Instrum. Method. Data Syst. Discuss., doi:10.5194/gi-2016-22, 2016
Manuscript under review for journal Geosci. Instrum. Method. Data Syst.
Published: 23 August 2016

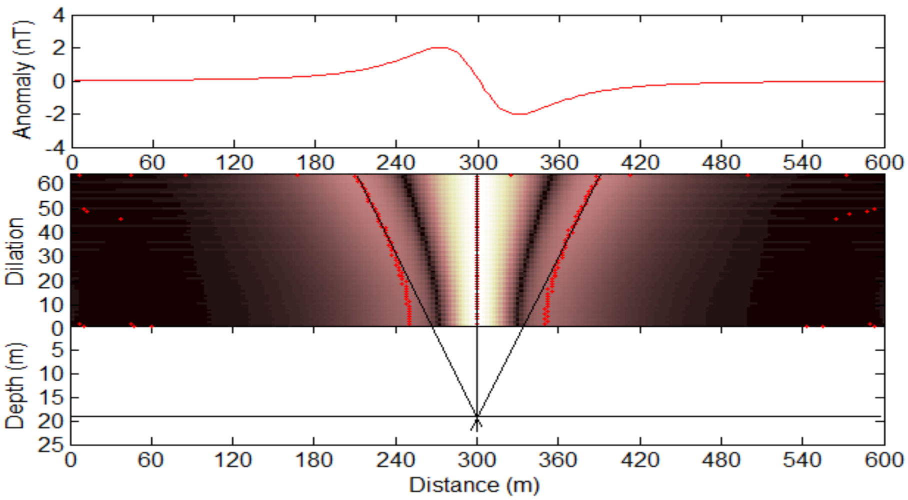

Figure 3: Synthetic magnetic anomaly of isolated extended source and depth estimation by Wavelet transform for a Poisson wavelet for γ=1 with mathematical expression $k(x) = -[x\,(2/\pi)]/\,(1+x^2)^2$.

The wavelet coefficients are computed by applying CWT to the anomaly. Fig. 4 shows the calculated values of CWT coefficients for different dilations (1-64.5) of magnetic anomaly. The maxima of modulus of CWT provide cone like structures and are clearly shown which points towards the position of the upper corner of the model. On the other hand, whereas an approximate horizontal location has been estimated, an intersection of modulus maxima lines in the subsurface has placed below the base line (a=0) to mark the depth of the source, where a is dilation.

Also, example illustrates the application of wavelet transform to potential fields (horizontal derivative, γ=1) makes a cone like shape and ridges of the cone join below the base line or to homogeneity centre of the source, where y-scale represents the dilation. The point where ridges joins mark the depth and location and of the vertical dipole. It is detected that homogeneous source retains a geometrical possession after execution of wavelet transform on potential field. This makes a straightforward interpretation about depth and location of causative body. In order to perform wavelet analysis on field data, it has been tested on noisy data with 1%, 2%, 5%, 10% noise in the potential source data obtained because of vertical dipole [Fig. 4 (a), (b), (c), (d)]. It is clear that Wavelet analysis provides the exact depth and location of the source.

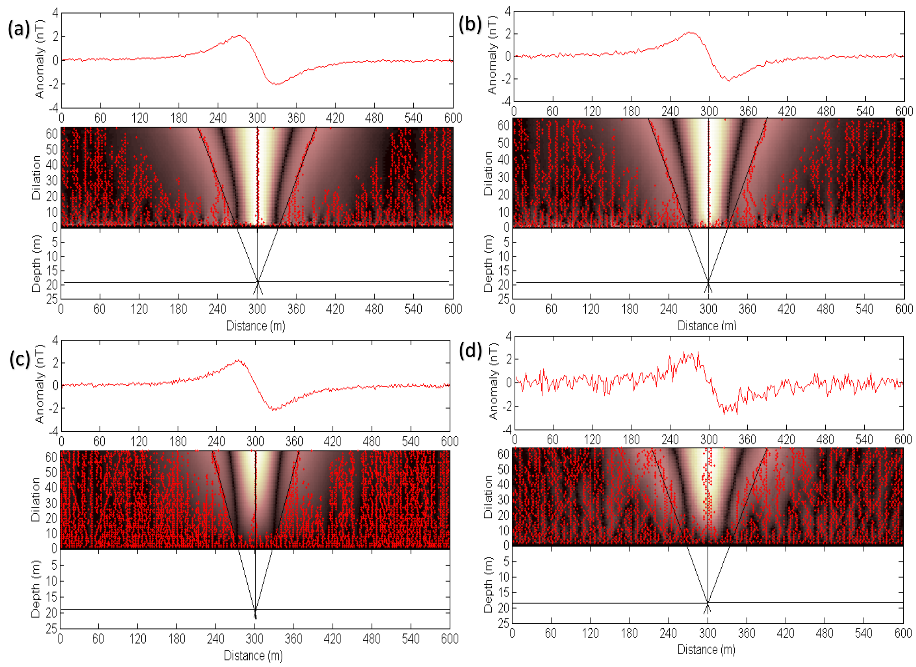

Figure 4: (a) magnetic anomaly with 1% noise (b) magnetic anomaly with 2% noise (c) magnetic anomaly with 5% noise (d) magnetic anomaly with 10% noise.

6. Application of CWT to magnetic field anomaly from Jharia coal field

The CWT and EDM are applied on field magnetic anomaly collected from Jharia Coal Field and surrounding regions, Dhanbad, India. For CWT analysis six profiles (AA', BB', CC', DD', EE' and FF') have been selected, which cover the entire coal field. Fig. 2 shows the magnetic anomaly map, in which a number of anomalous sources such as extension, direction of the bodies, geological faults/fold and tectonic signature has been shown. These anomalies can be adequately explained by assuming an underlying body having susceptibility contrast with respect to its surroundings and which is polarized in N-S direction. The positive anomaly in the northern part of the basin is clearly seen in the profile.

The Remanence or remanent magnetization or residual magnetism of the body also appears to contribute to the anomaly. It is interesting to note that in the region of this magnetic anomaly a number of dykes and sills are found to be intrusive into the sediments as shown in Fig 2. This anomaly therefore could be ascribed to the presence of a basic or ultrabasic body which could be source for the basic dykes and sills which intruded into the basin during Gondwana times. Alternatively, this anomaly could also represent a basic intrusive of Precambrian age underlying the sediments. There are practically no basic intrusive present in the region of positive anomaly. Therefore, this anomaly could be more definitely ascribed to an intrusive body of Precambrian age Verma et al. (1979).

7. Results and discussion

In order to check the reliability of the interpreted results obtained from Euler deconvolution, CWT and geological sections construction information collected from published results of boreholes drilled by Geological Society of India (G.S.I.), Bharat Coking Coal Limited (B.C.C.L.), National Coal Development Corporation (N.C.D.C.), Central Mines Planning and Design Institute (C.M.P.D.I). Therefore, the depth to the basement configuration inferred from gravity data as well as drilled borehole information discussed below.

Jharia coalfield and surrounding areas have been considered to estimate the source depths on the basis of technique of intersections of modulus maxima lines of CWT. The mean depths of causative sources along the profile AA′ (passes east of the Khanudih and west of the Telmuchu and Bansjora region through Amdih over western most part of the Jharia coal field, shown in Fig. 2) calculated from the CWT [Fig. 5 (i) (a)] and Daubechies wavelet method [Fig. 5 (i) (b)] varies from 0.2 km to 0.45 km. Profile AA′ shows that there is fault near the north-western part of the basin.

Magnetic Field Inclination, Declination and Azimuth Angle (clockwise from True North) of this profile are 36.44°, -0.11° and 268.48° respectively. Anomaly hike about 77 nT between borehole JM-4 and JK-26 has been observed because of a number of basic intrusive bodies belong to Satpura cycle exist over the area. Jharia coalfield consist of peridotites in the forms of sills as well as dykes. Dolerite dykes are very common in western part of this coalfield.

Central part shows flat sedimentary region and magnetic anomaly shows high value on either side of the profile. Raniganj formation exists on southern side whereas Talchir formation exists on the northern side of this profile. However, the Barren-Measures and the Barakar formations are lies in between the Raniganj and the Talchir formations. There is an intrusion of Archean metamorphics in Talchir formation which shows as outcrop over the surface near Amdih [Fig 5 (ii)]. The some of the bore holes provide the information about the metamorphics along this profile. The maximum thickness of the sediment along this profile is observed about 0.8 km.

Bore holes JM-1, JM-4 and JK-26 are located close to this profile, which touches metamorphics at the depth about 0.4 km 0.55 km and 0.3 km respectively. These bore hole are located west of Bansjora and Telmuchu. The depth to the basement obtained from magnetic data is nearly equal to the depth obtained from gravity data along these profiles (Singh and Singh, 2015).

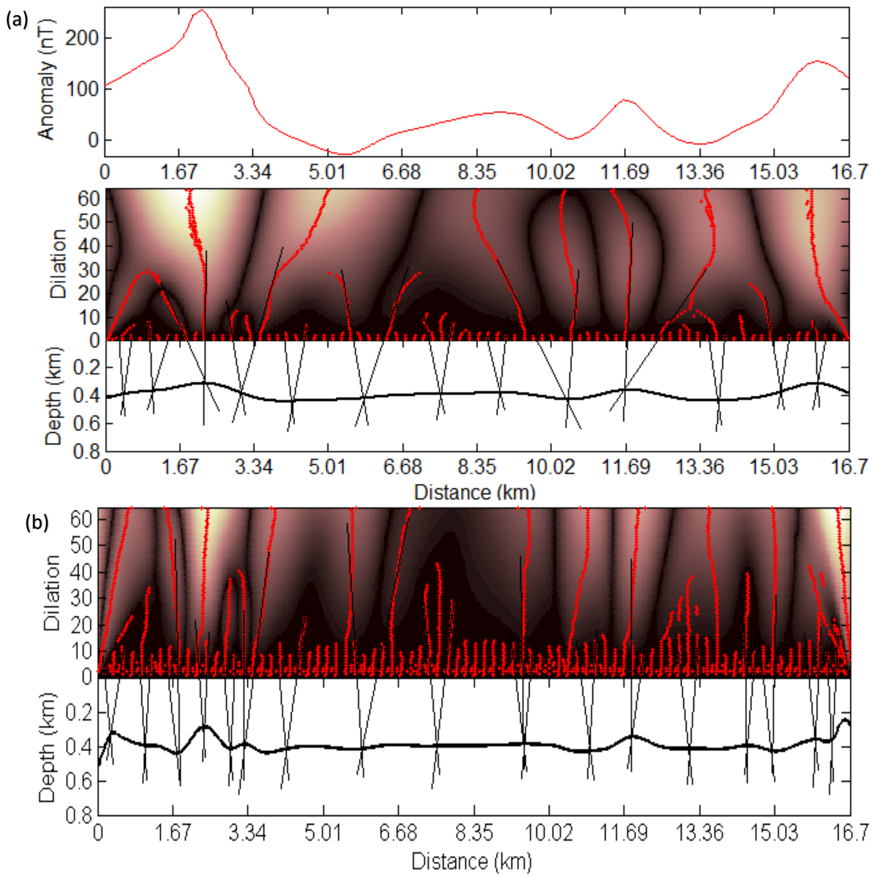

Figure 5 (i): (a) Magnetic anomaly across the profile AA′ (drawn in Fig. 2) and depth estimation by Continuous Wavelet Transform, (b) Depth estimation by Daubechies wavelet.

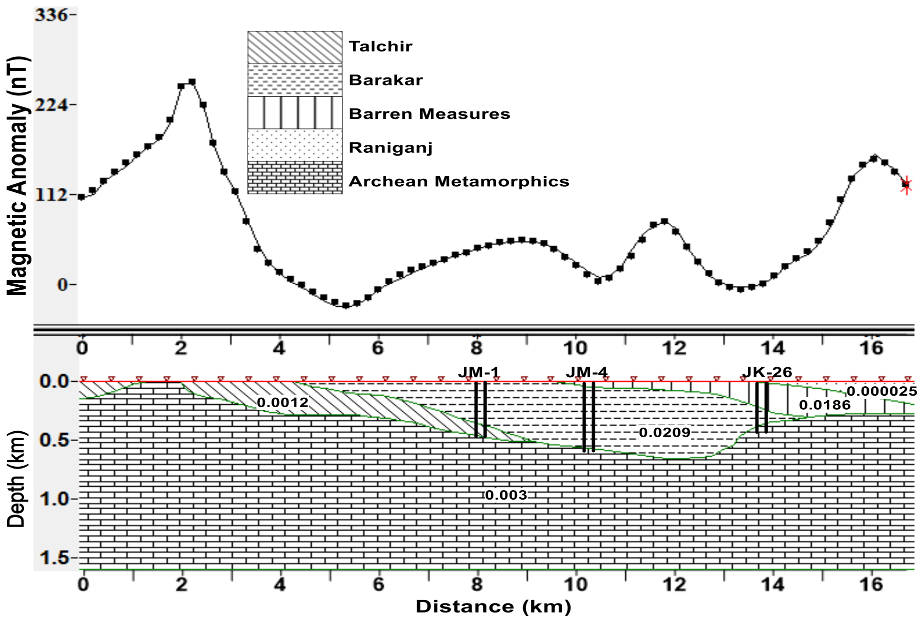

Figure 5 (ii): 2D-model of the Profile AA′ drawn in Fig. 2.

The mean depths of causative sources along the profile BB′ (passes east of Telmuchu and Bansjora and west of Kumardih region, shown in Fig. 2) calculated from the CWT [Fig. 6 (i) (a)] and Daubechies wavelet [Fig. 6 (i) (b)] varies from 1.3 km to 2.5 km. Central part of the basin shows the abrupt changes in the magnetic anomaly.

Profile BB′ illustrates about the Barakar, the Raniganj, the Talchir and the Barren-Measures. The barren measures is found in between the Barakar and Raniganj formation which shows the outcrops in both sides of the Raniganj formation. Also, there is an intrusion of Talchir formation has been found in Archean metamorphics and Barakar formation at northern end of the profile [Fig. 6 (ii)]. There is a sloppy nature exist on both side of the profile. The major portion of this area is dominated by the Raniganj and the Barakar formations. The estimated thickness of the sediments is about 2.3 km over the Raniganj formation.

Magnetic Field Inclination, Declination and Azimuth Angle of this profile are 36.42°, -0.11° and 268.5° respectively. This profile passes through two faults between metamorphics and sediment, one is at southern end while another one at northern end of the profile. Faults are indicated by steep gradient of magnetic anomaly. There are Gondwana basin trapes are normally magnetized. Raniganj formation infested with numerous dykes and sills. Magnetic anomaly hike about 103 nT and 162 nT south east and east of Bansjora represent the occurrence of Precambrian basement underlying he sediments.

Geological section along this profile BB′ is deduced from analysis of gravity data, available geological information and bore hole information. The bore hole JK-7 and JM-8 are located near this profile. From the bore hole JM-7, it is obtained that maximum thickness of the Raniganj formation is about 0.220 km and Barren-Measures lies below it. It touches the Barakar formation at the depth about 1.2 km near east of Bansjora. Obtained results from JK-8, it is clear that sediment thickness is about 0.3 km and bore hole touches the Barren-Measures at the depth about 300 m.

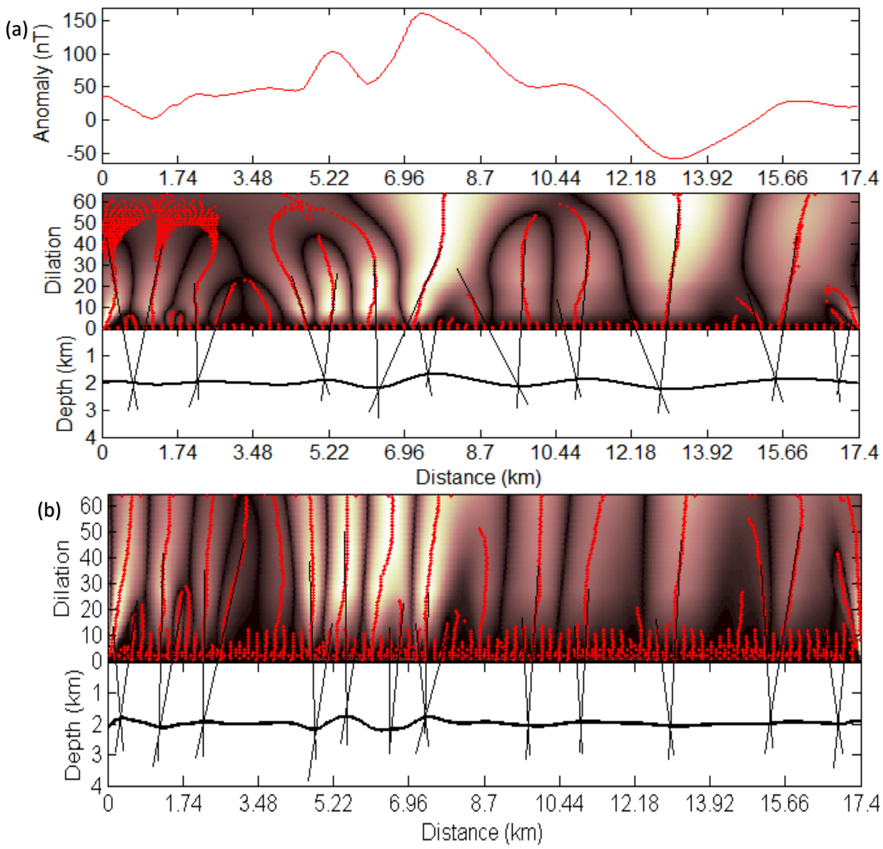

Figure 6 (i): (a) Magnetic anomaly across the profile BB′ and depth estimation by Continuous Wavelet Transform, (b) Depth estimation by Daubechies wavelet.

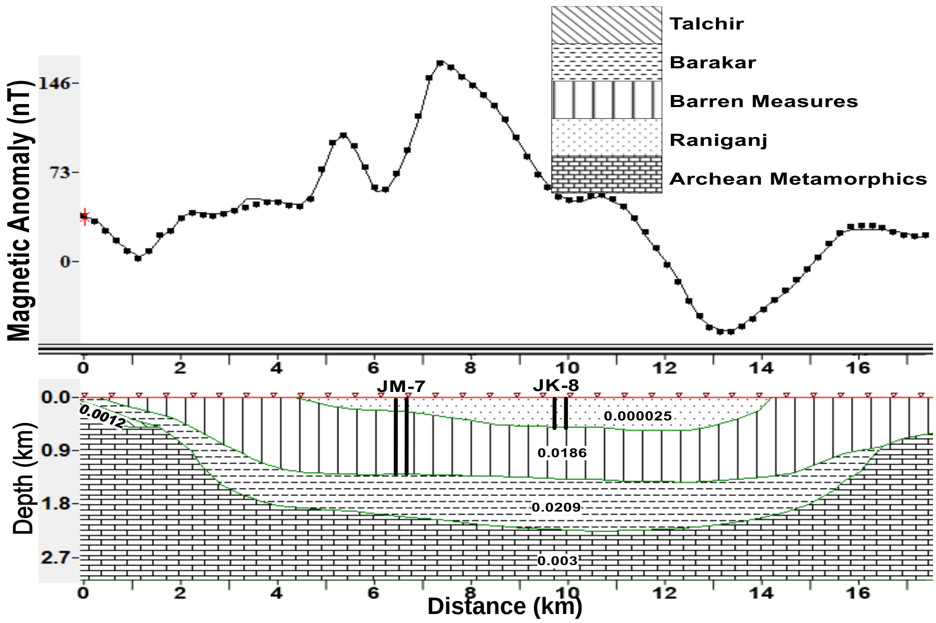

Figure 6 (ii): 2D-model of the Profile BB′ drawn in Fig. 2.

The mean depths of causative sources along the profile CC′ (passes west of Mahuda and Katras through Kumardih region, shown in Fig. 2) calculated from the CWT [Fig. 7 (i) (b)] and Daubechies wavelet method [Fig. 7 (i) (b)] varies from 1 km to 2 km. Northern part of the basin shows the flatness in the basin. Most of the sedimentary formations exist along the profile CC′. [Fig. 7 (ii)] reveals that there is a strong indication of both boundaries have slope towards the central part of the basin and the southern boundary is categorized by an abrupt slope than the northern.

Magnetic Field Inclination, Declination and Azimuth Angle of this profile are 36.41°, -0.12° and 268.516° respectively. Gee (1932) mentioned four dykes in the memoir of this coalfield, namely Salama dyke, Sitarampur dyke, Charanpur dyke and Barakar river dyke. The flow of the Barakar river has been shown in Fig. 1. It is remarkable that in this region of this magnetic anomaly profile numbers of ultrabasic dyke (mica peridotites) and sills are found as intrusive into sediments and Barakar formation causes magnetization of the body in the presents earth's field.

Similar to the Profile BB′ Barren measures lies between the Raniganj and Barakar formation. Also, Talchir formation lies between the Barakar and Archean metamorphics whose thickness varies about 1.8 km to 2.2 km at north central part of the basin. The thickness of sediments near Kumardih and Mahuda is about 2.4 km. Moreover, geological sections along the profile CC′ is also based on the results obtained from gravity data, bore hole information as well as geological information. Bore hole NCJA-4, NCJA-5 and MN-11 are located near this profile. Bore hole NCJA-4 and NCJA-5 are located south west of Katras and north east of Kumardih. Depth analysis of individual formation near deepest part of the basin are about 0.4 km for Raniganj formation, 0.95 km for Barren-Measures, 0.8 km for Barakar formation and about 0.2 km for Talchir formation.

Geosci. Instrum. Method. Data Syst. Discuss., doi:10.5194/gi-2016-22, 2016
Manuscript under review for journal Geosci. Instrum. Method. Data Syst.
Published: 23 August 2016

Geoscientific Instrumentation Methods and Data Systems
Discussions
Open Access

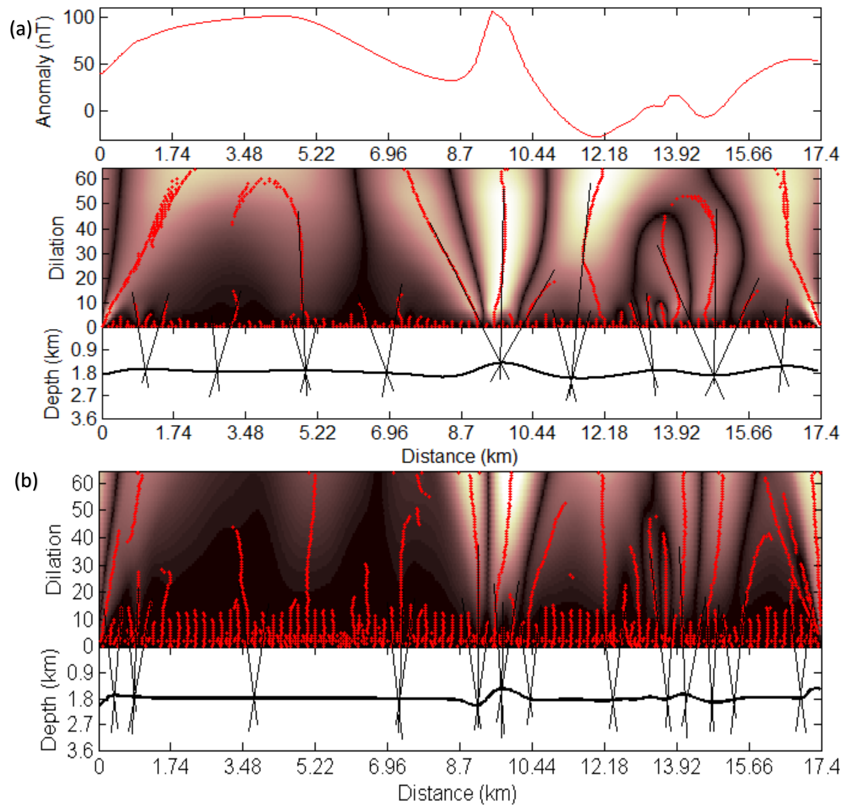

Figure 7 (i): (a) Magnetic anomaly across the profile CC′ (drawn in Fig. 2) and depth estimation by Continuous wavelet transform, (b) Depth estimation by Daubechies wavelet.

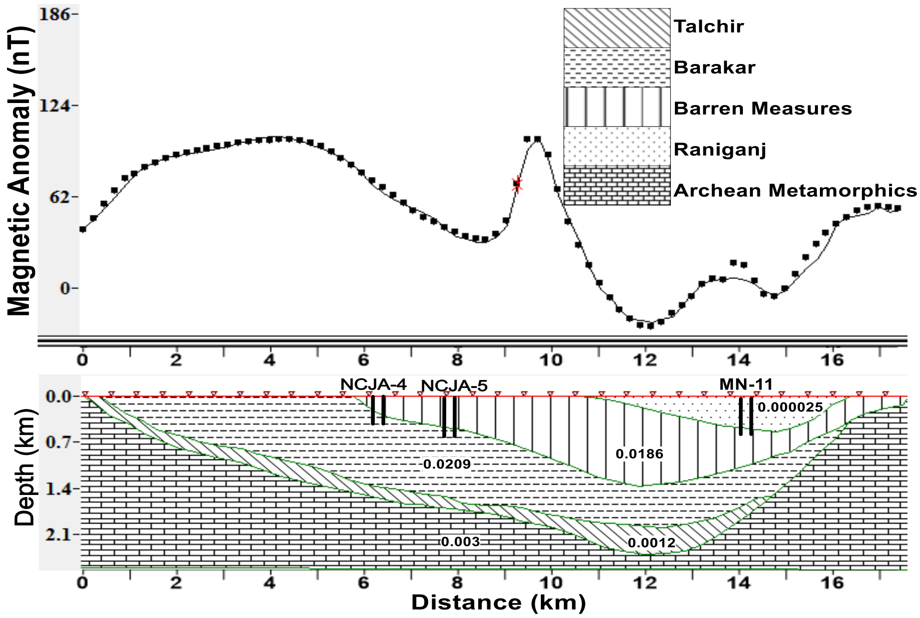

Figure 7 (ii): 2D model of the Profile CC′ drawn in Fig. 2.

The mean depths of causative sources along the profile DD′ (passes east of Mahuda and Katras and west of Parbatpur and Dubrajpur though Barki region, shown in Fig. 2) calculated from the CWT [Fig. 8 (i) (a)] and Daubechies wavelet method [Fig. 8 (i) (b)] varies from 1 km to 2.4 km. Also, along this profile there are some indication of fractious contact between the Barakar formation and Barren Measures. Barakar formation appear to pinch out close to the southern boundary fault.

Magnetic Field Inclination, Declination and Azimuth Angle of this profile are 36.40º, -0.12º and 268.529º respectively. Fault between Barakar formation and metamorpics are clearly indicated by steep gradients of magnetic anomaly at northern end of profile. Southern end of the profile characterized by magnetic variation appears due to an uneven topography. Middle of the profile characterized by a magnetic high of about 151 nT because of two dimensional linear feature and magnetic pole which lies nearly 0.5-0.65 km below the surface in this region. The extent of Talchir formation assumed to be underlying the Barakar formation is uncertain. Some coal seams exhibit on the surface and northern side have the steep dip than the southern side. Approximate depth of the basement in this area estimated due to single pole at depth of about 2.0 km [Fig. 8 (ii)] below the surface near south west of Parbatpur.

Geological sections along this profile also deduced from the analysis of bore hole information, gravity data and geological information. Bore hole NCJA-14, JK-5 and NCJP-32 are located south of Phalmahul, north west of Dubrajpur and west of Parbatpur respectively. The individual maximum thickness of various formations near deepest part of the of the basin are about 0.8 km for Talchir, 0.4 km for Barren-Measure and about 2 km for Barakar formation.

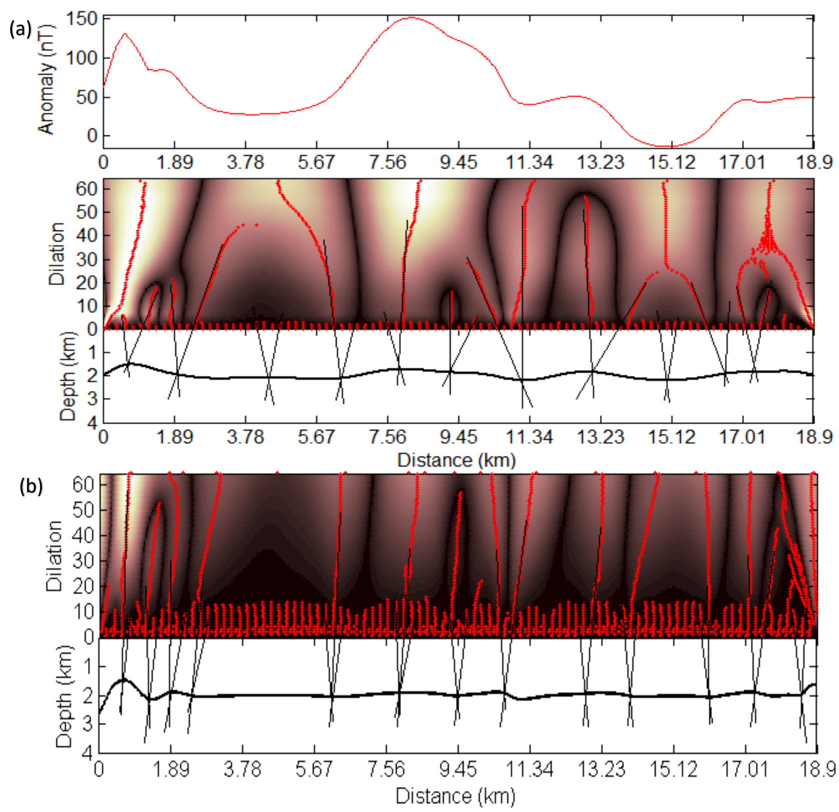

Figure 8 (i): (a) Magnetic anomaly across the profile DD′ (drawn in Fig. 2) and depth estimation by Continuous Wavelet Transform. (b) Depth estimation by Daubechies wavelet.

Geosci. Instrum. Method. Data Syst. Discuss., doi:10.5194/gi-2016-22, 2016
Manuscript under review for journal Geosci. Instrum. Method. Data Syst.
Published: 23 August 2016

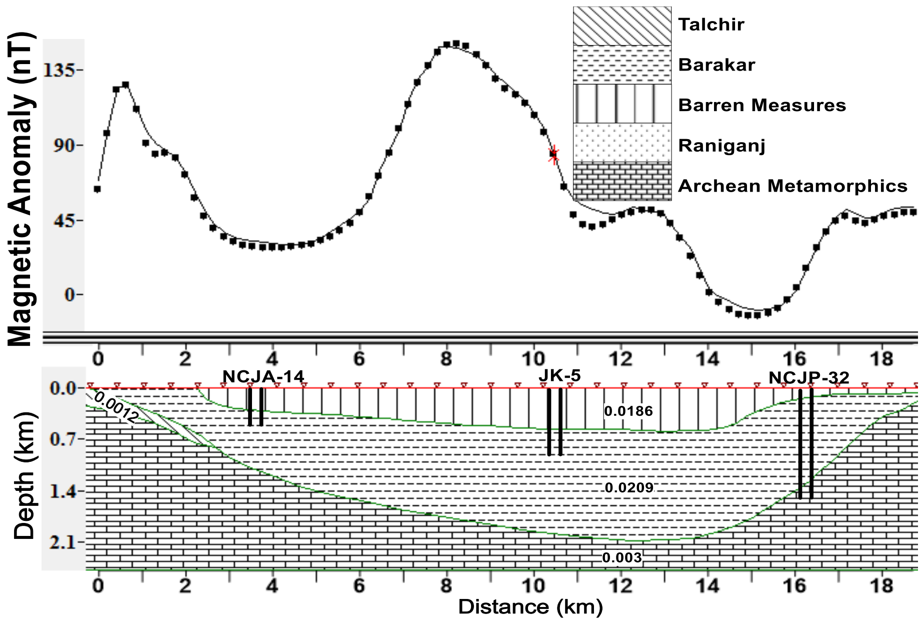

Figure 8 (ii): 2D model of the Profile DD′ drawn in Fig. 2.

The mean depths of causative sources along the profile EE′ (passes east of the Parbatpur and Dubrajpur and west of Dungri, Kustore region, shown in Fig. 2) calculated from the CWT [Fig. 9 (i) (a)] and Daubechies wavelet [Fig. 9 (i) (b)] varies from 1.8 km to 2.8 km. There is a gentle slope of the basin on the northern side, uplift of the basement in the southern part and steep slope close to the southern boundary fault is clearly indicated in this profile.

Magnetic Field Inclination, Declination and Azimuth Angle (clockwise from True North) of this profile are 36.39º, -0.12º and 268.556º respectively. Anomaly over this profile can be adequately explained because underlying body having susceptibility contrast with respect to its surrounding. The depth of the basement near the top pole is estimated about 1.5-1.6 km from the surface. Anomaly hike at the middle of the profile could be ascribed to the presence of basic or ultrabasic body which was a source for sills and basic dykes which intruded into basin during Precambrian age. The south pole of the underlying source is found to be at a depth of about 0.4 km and the north-pole at 0.7 km depth below the surface [Fig. 9 (ii)]. Eastern margin shows the impact of the occurrence of some faults and extension of metamorphic runs under the sediments up to distance of about 1.12 km.

Geological section along this profile are also deduced from the gravity data, bore hole information and available geological informations. Individual thickness of each formation is also deduced with the help of bore holes JK-4, NCJP-42, NCJP-16 and NCJP-12 which are located south west of Kustor, west of Nunikdih, west of Dungri and south of Dungri respectively. Maximum thickness is about 0.45 km for Barren-Measures, about 1.5 km for Talchir and 1.4 km for Barakar formation have been inferred.

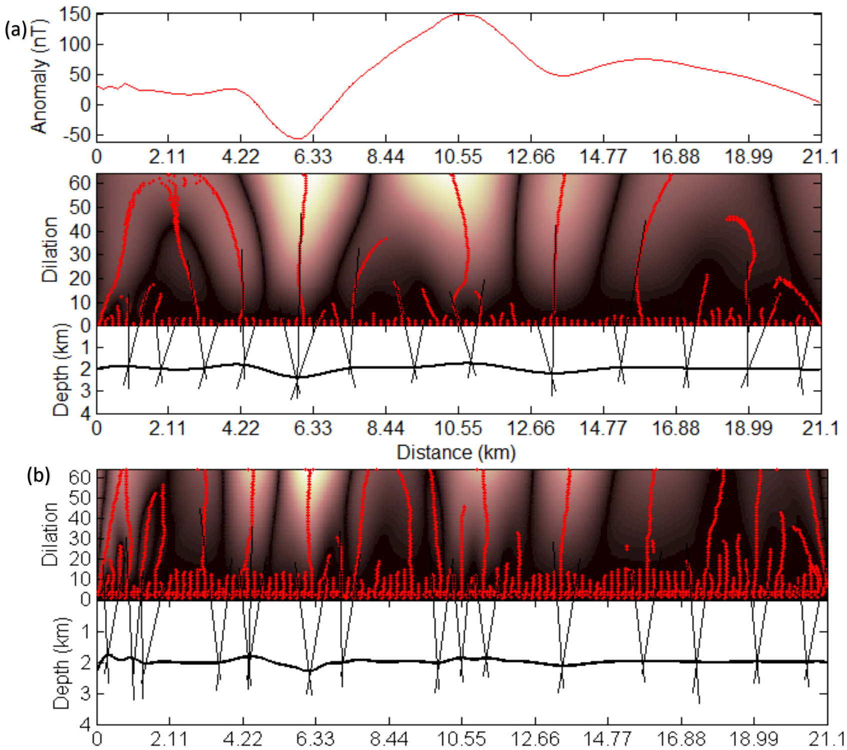

Figure 9 (i): (a) Magnetic anomaly across the profile EE′ (drawn in Fig. 2) and depth estimation by Continuous Wavelet Transform. (b) Depth estimation by Daubechies wavelet.

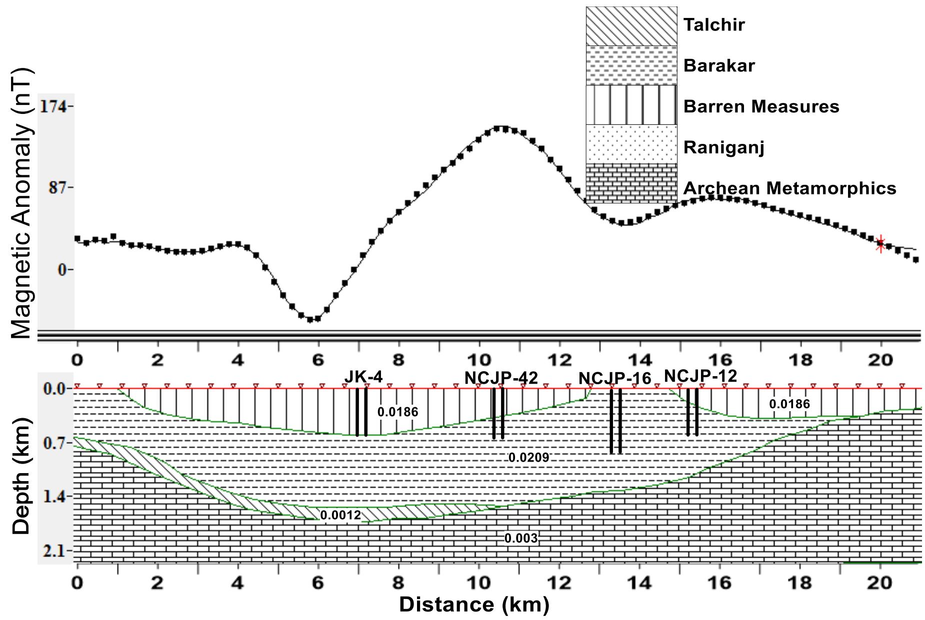

Figure 9 (ii): 2D model of the Profile EE′ drawn in Fig. 2

The mean depths of causative sources along the profile FF′ (passes east of the Jharia, Dhanbad and west of the Makunda and Pathardih region, shown in Fig. 2) calculated from the CWT [Fig. 10 (i) (a)] and Daubechies wavelet method [Fig. 10 (i) (b)] varies from 1 km to 2.5 km. Also, magnetic anomaly suggest that this area is geologically highly disturbed and dips of the formations varies rapidly.

Magnetic Field Inclination, Declination and Azimuth angle of this profile are 36.33º, -0.13º and 268.584º respectively. Patherdih horst which is tongue of gneisses penetrates the south east corner of this region. There are strong faults occurs at both ends of the profile. Several interesting possibilities arise regarding the basic intrusives of dykes as well as schists which are normally magnetized. The hike in the anomaly of about 110 nT at middle of the profile is due to Peridotite dykes and sills having the close association with Barren-Measure and Barakar formation.

It is found that in this region of magnetic anomaly remanent magnetization of the body also appears to contribute to the magnetic anomaly. A number of sills and ultrabasic dykes (mica peridotites) are found to be intrusive into the sediments. Geology over this

Geosci. Instrum. Method. Data Syst. Discuss., doi:10.5194/gi-2016-22, 2016
Manuscript under review for journal Geosci. Instrum. Method. Data Syst.
Published: 23 August 2016

Geoscientific Instrumentation Methods and Data Systems Discussions

profile could be described to the presence of a basic or ultrabasic body which was main source for the sills and basic dykes intruded [Fig. 10 (ii)] into the basin during Gondwana times (Verma et al., 1973).

Geological strata along this profile are highly disturbed. Therefore, dip of the formations varies abruptly. The thickness of the formations is extrapolated from gravity data, bore holes NCJB-9, NCJB-25 and JFT-8 information as well as geological information. Bore hole NCJB-9, NCJB-25 and JFT-8 are located west of Chhatabad, west of Patherdih and west of Bhojudih respectively. Borehole JFT-8 has the cross contact between Barren-Measures and Barakar formation and it touches the metamorphics at about 0.4 km near west of Bhojudih. The depth of the individual formations are approximately equal to the depth obtained from interpretation of gravity data (Singh and Singh, 2015).

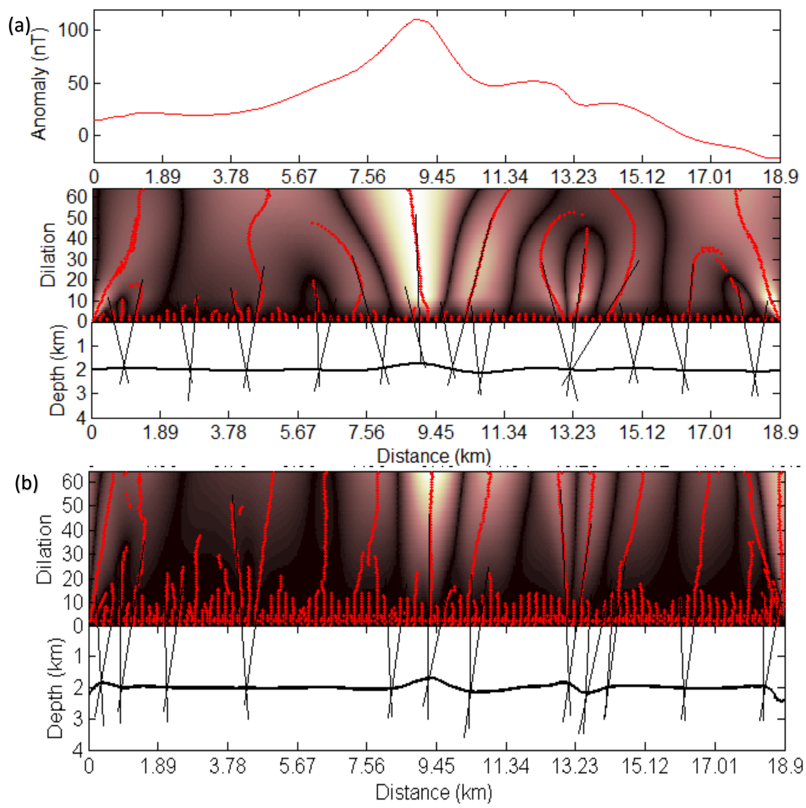

Figure 10 (i): (a) Magnetic anomaly across the profile FF′ (drawn in Fig. 2) and depth estimation by Continuous Wavelet Transform. (b) Depth estimation by Daubechies wavelet.

Geosci. Instrum. Method. Data Syst. Discuss., doi:10.5194/gi-2016-22, 2016
Manuscript under review for journal Geosci. Instrum. Method. Data Syst.
Published: 23 August 2016

Geoscientific Instrumentation Methods and Data Systems
Open Access
Discussions

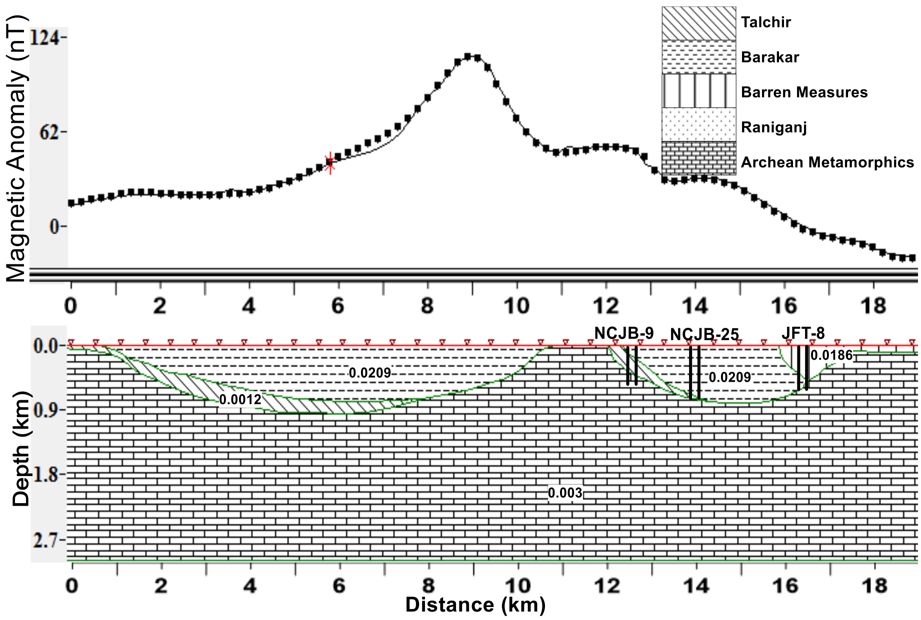

Figure 10 (ii): 2D model of the Profile FF′ drawn in Fig. 2

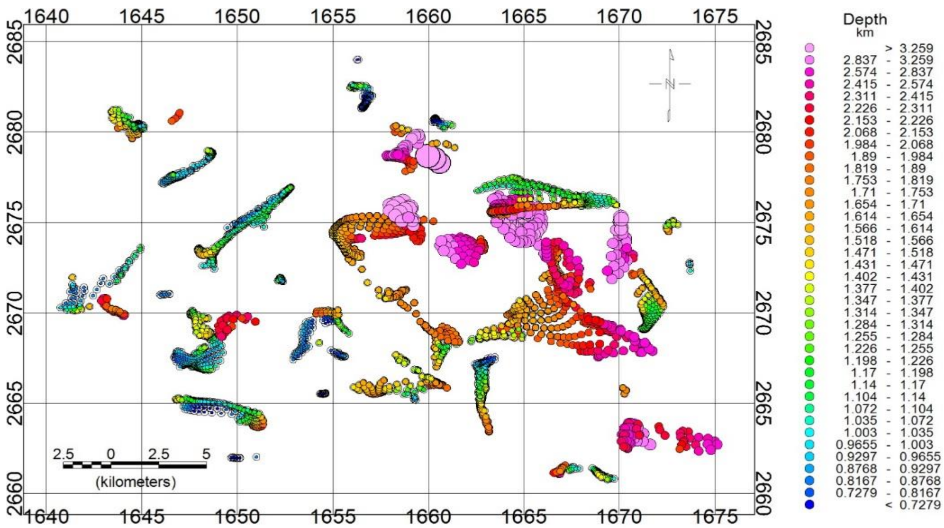

Figure 11: The depth estimates obtained from Euler deconvolution (SI=2) are plotted over UTM coordinates of the study region.

The interpretation of magnetic anomaly over Jharia coalfield compared with some information from interpretation of gravity data (Verma and Ghosh, 1974). The mean depth to the causative sources of magnetic anomaly estimated by Euler deconvolution method (Fig. 11) ranges about 0.6 km to 3.2 km. The mean depth of the profiles has been shown in the table 1.

Algorithm of Euler deconvolution to the total magnetic field anomaly from the Jharia coalfield (Fig. 2). The magnetic field anomaly is predominantly due to irregular fluctuation of Precambrian outcrops and faults. The magnetic data are sampled at roughly 50 m along the profile direction. To enhance the signal to noise ratio, a high cut filter was applied in the wavenumber domain and partial derivative in the vertical direction was obtained by extending the field grid before the calculation. The SI is supposed to vary between 0 and 3 covering all plausible geological bodies. The estimates of source location and depth are obtained by minimizing the error function using nonlinear optimization technique of Coleman and Li (1996).

Fig. 11 shows two sets of fractures, predominantly oriented in the NE and SE at northern and southern boundary respectively. The orientation of fracture set agrees with the orientation obtained from regional magnetic interpretation (Verma et al. 1973). In the southern region, the depth of the Precambrian basement derived from the faults is less than that in the northern region. Furthermore, intense fracturing is detected in the centre of the study area. In the western and southern region, the source depth is shallow compared to that of the eastern and northern region.

It suggesting that the most of sediments lies below 700 m, which is reasonable as calculated by wavelet transform method. The intense fracturing at the both north and south boundary grid produces sharp basement between them as observed in the bathymetry. Thus, the faults and depths obtained from the Euler deconvolution, CWT and Daubechies wavelet are related to each other as results obtained from the regional magnetic interpretation.

Geosci. Instrum. Method. Data Syst. Discuss., doi:10.5194/gi-2016-22, 2016
Manuscript under review for journal Geosci. Instrum. Method. Data Syst.
Published: 23 August 2016

Table 1: Mean depth of sources calculated from magnetic anomaly by CWT and Daubechies wavelet along the profiles drawn over Jharia coal field and surrounding regions.

Name of Profiles	Distance with depth (km)						
	3	6	9	12	15	18	21
AA′	0.3	0.4	0.38	0.37	0.39	-	-
BB′	2	2.4	2.2	2.5	1.8	-	-
CC′	1.6	1.7	1.2	1.9	2	-	-
DD′	2.2	2.8	1.7	1.8	2.3	-	-
EE′	1.8	2.8	1.8	2	1.7	1.9	2.1
FF′	2.1	2.2	1	1.7	1.8	-	-

Table 2: The following Magnetic susceptibility used to prepare the geological sections. Susceptibility values are taken from the standard chart compiled by Clark and Emerson (1991) and Hunt et al. (1995).

Formation	**Litho-type**	**Susceptibility (SI unit)**
Raniganj	Fine grained feldspathic sandstones, shales with coal seams	Sandstone=0.0209 Shale=0.0186 Coal=0.000025
Barren Measures	Buff- coloured sandstones, shales and carbonaceous shales	Sandstone=0.0209 Shale=0.0186
Barakar	Buff-coloured coarse and medium-grained feldspathic sandstones, carbonaceous shales, fire clays and coal seams	Sandstone=0.0209 Shale=0.0186 Clay=0.00025 Coal=0.000025
Talchir	Silt, Carbonates Greenish shale and fine grained sandstones	Silt/Carbonates=0.0012 Shale=0.0186 Sandstone=0.0209
Metamorphics	Granite Gneisses, quartzites, mica schists and amphibolites	Granite=0.05 Gneisses=0.025 Quartzites=0.0044 Mica schists=0.003 Amphibolites=0.00075

8. Conclusions

It has been shown that CWT allows estimation of the position of the buried source anomalies. For large dilations, the modulus maxima of the CWT and Daubechies wavelet of the magnetic anomalies contain the main features of the location and depth information of anomalous body in the magnetic anomaly. The study over Jharia coal field proves the CWT and Daubechies wavelet method are very efficient to explain the positions of causative sources of potential field (magnetic) data. Extrema lines of these wavelet transforms give satisfactory and reliable informations required to enhance the key parameters of the sources depth and locations.

The application of the CWT to the synthetic and field magnetic data over Jharia coal fields and surrounding regions demonstrates that the CWT and Euler deconvolution [Fig. 16] methods are rapid, easy to execute. Mean depth of causative sources of potential field data obtained from CWT can help to improve qualitative and quantitative interpretation. Also, CWT and Euler deconvolution provide shape of causative sources without any prior knowledge. These methods can play an important role in constructing initial models required for 2-D and 3-D or joint inversion of gravity and magnetic anomalies with better accuracies in very short period.

9. References

Ardestani, E. V., 2010, Precise Edge detection of gravity anomalies by Tilt angle filters, Journal of the Earth & Space Physics, 36, 2, 11-19.

Barbosa, V. C. F., Silva, J. B. C. and Medeiros, W. E., 1999, Stability analysis and improvement of structural index estimation in Euler deconvolution, Geophysics, 64, 48-60.

Blakely, R.J., and Simpson, R.W., 1986, Approximating edges of source bodies from magnetic or gravity anomalies, Geophysics, 51 (7), 1494-1498.

Bhattacharyya, B. P., 1972, Tectono-metamorphic effect of granite and pegmatite emplacement in the Precambrian of Bihar Mica Belt. Proc. Symp. On Metallogeny of the Precambrian. Geological Society of India, Bangalore 45-56.

Bott, M. H. P. and Ingles, A., 1972, Matrix methods for joint interpretation of two-dimensional gravity and magnetic anomalies with application to the Iceland- Faeroe Ridge, Geophys. J. Roy. Astr. Soc., 30, 55-67.

Chamoli, A., Srivastava, R. P. and Dimri, V. P., 2006, Source depth characterization of potential field data of Bay of Bengal by continuous wavelet transform, Indian Journal of Marine Sciences, 35(3), 195-204.

Clark, D.A., and Emerson, D.W., 1991, Notes on rock magnetization characteristics in applied geophysical studies, Exploration Geophysics, 22, 547-55.

Cooper, G. R. J., 2004, A semi-automatic procedure for the interpretation of geophysical data, Exploration Geophysics, 35, 180-185.

Cooper, G. R. I. and Cowan, D. R., 2006, Enhancing potential field data using filters based on the local phase, Comp. & Geoscience, 32, 1585-1591.

Cooper, G. R. J. and Cowan Duncan R., 2008, Edge enhancement of potential field data using normalized statistics, Geophysics, 73(3), H1-H4.

Cooper, G. R. J., 2011, The semiautomatic interpretation of gravity profile data. Comp. & Geoscience, 37, 1102-1109.

Geosci. Instrum. Method. Data Syst. Discuss., doi:10.5194/gi-2016-22, 2016
Manuscript under review for journal Geosci. Instrum. Method. Data Syst.
Published: 23 August 2016

Coleman, T. F. and Y. Li., 1996, An interior, trust region approach for nonlinear minimization subject to bounds, SIAM J. on Optimization, 6, 418-445.

Dewangan, P., Ramprasad, T., Ramana, M. V., Desa, M. and Shailaja, B., 2007, Automatic interpretation of magnetic data using Euler deconvolution with nonlinear background, Pure and Applied Geophysics, 164, 2359-2372.

Fernández Martínez, J. L., Fernández Muñiz, Z., Pallero, J. L. G., Pedruelo González, L. M., 2013, From Bayes to Tarantola: New insights to understand uncertainty in inverse problems, Journal of Applied Geophysics, 98, 62-72.

Fernández Martínez, J. L., Fernández Muñiz, M. Zulima., Tompkins, Michael J., 2012, On the topography of the cost functional in linear and nonlinear inverse problems, Geophysics, 77, W1-W15.

FitzGerald, D., Reid A., and McInerney, P., 2004, New discrimination techniques for Euler deconvolution, Comp. & Geoscience, 30, 461-469.

Fox, C. S., 1930.The Jharia Coal Field, Geological Survey of India, Memoir, 56, 253.

Gallardo Delgado, L. A., Perez Flores, M. A. and Gomez Trevino, E., 2003, A versatile algorithm for joint 3D inversion of gravity and magnetic data, Geophysics, 68, 949-959.

Gerovska, D. and Arauzo Bravo, M. J., 2003, Automatic interpretation of magnetic data based on Euler deconvolution with unprescribed structural index, Comp. & Geoscience, 29, 949-960.

Gee, E. R., 1932, The geology and coal resources of the Raniganj coalfield, Mem. Geol. Surv. India, 61, 1-343.

Goyal, P. and Tiwari, V. M., 2014, Application of the continuous wavelet transform of gravity and magnetic data to estimate sub-basalt sediment thickness, Geophysical Prospecting, 62, 148-157.

Gunn, P. J., 1975, Linear transformations of gravity and magnetic fields, Geophysical Prospecting, 23, 300-312.

Hunt, C. P., Moskowitz, B.M. and Banerjee, S.K., 1995, Magnetic properties of Rocks and Minerals, In: Rock Physics and Phase Relations - A hand book of Physical constants, AGU Reference shelf 3, etd. Ahrens, T. J., 189-204.

Hsu, S. K., Sibuet, J. C. and Shyu, C. T., 1996, High resolution detection of geologic boundaries from potential-field anomalies: an enhanced analytic signal: technique, Geophysics, 61, 373-386.

Hsu, S. K., 2002, Imaging magnetic sources using Euler's equation, Geophysical Prospecting, 50, 15-25.

Holschneider, M., A. Chambodut, and M. Mandea, 2003, From global to regional analysis of the magnetic field on the sphere using wavelet frames, Physics of the Earth and Planetary Interiors, 135, 107-124.

Jiang Fan, Wu Jiansheng and Wang Jialin, 2008, Joint inversion of gravity and magnetic data for a two-layer model, Applied Geophysics, 5, 331-339.

Keating, P. B., 1998, Weighted Euler deconvolution of gravity data, Geophysics, 63, 1595-1603.

Kopal, Z., 1961, Numerical analysis, Chapman and Hall Ltd., London, 551-553.

Melo, F. F., Barbosa, V. C. F., Uieda, L., Oliveira Jr, V. C. and Silva, J. B. C., 2013, Estimating the nature and the horizontal and vertical positions of 3D magnetic sources using Euler deconvolution, Geophysics, 78, J87-J98.

Menichetti, V., and Guillen, A., 1983, Simultaneous interactive magnetic and gravity inversion, Geophysical Prospecting, 31, 929-994.

Moreau, F., Gibert, D., Holschneider, M. and Saracco, G., 1997, Wavelet analysis of potential fields, Inverse Problems, 13, 165-178.

Moreau, F., Gibert, D., Holschneider, M., and Saracco, G., 1999, Identification of sources of potential fields with continuous wavelet transform: Basic theory, Journal of Geophysical Research, 104, 5003-5013.

Mushayandebvu, M. F., Van, Driel P., Reid, A. B., and Fairhead, J. D., 2001, Magnetic source parameters of two dimensional structures using extended Euler deconvolution, Geophysics, 66, 814-823.

Mushayandebvu, M. F., Lesur, V., Reid, A. B., and Fairhead, J. D., 2004, Grid Euler deconvolution with constraints for 2D structures, Geophysics, 69, 489-496.

Perez, Wijns, C. C. and Kowalczyk, P., 2005, Theta map: Edge detection in magnetic data: Geophysics, 70(4), L39-L43.

Pilkington, M., 2006, Joint inversion of gravity and magnetic data for two layer models, Geophysics, 71, 35-42.

Raja Rao, C. S., 1987, Coalfield of India, v.IV (pt.1) Bull. Geol. Surv. India, Series A, 45, 336.

Ravat, D., 1996, Analysis of the Euler method and its applicability in environmental investigations, Journal of Environmental and Engineering Geophysics, 1, 229-238.

Reid, A. B., Allsop, J. M., Granser, H., Millet, A. J. and Somerton, I. W., 1990, Magnetic interpretation in three dimensions using Euler deconvolution, Geophysics, 55, 80-91.

Reid, A. B., Ebbing, J. and Webb, S. J., 2014, Avoidable Euler Errors- the use and abuse of Euler deconvolution applied to potential field, Geophysical Prospecting, 62, 1162-1168.

Salem, A., Williams, S., Fairhead, J. D., Ravat, D. and R. Smith, 2007, Tilt-depth method: a simple depth estimation method using first order magnetic derivatives, The Leading Edge, 26/12, 1502-1505.

Sailhac, P., Gibert, D. and Boukerbout, H., 2009, The theory of the continuous wavelet transform in the interpretation of potential fields: A review, Geophysical Prospecting, 57, 517-525.

Silva, J. B. C., Barbosa, V. C. F. and Medeiros, W. E., 2001, Scattering, symmetry, and bias analysis of source position estimates in Euler deconvolution and its practical implications, Geophysics, 66, 1149-1156.

Geosci. Instrum. Method. Data Syst. Discuss., doi:10.5194/gi-2016-22, 2016
Manuscript under review for journal Geosci. Instrum. Method. Data Syst.
Published: 23 August 2016

Silva, J. B. C. and Barbosa, V. C. F., 2003, 3D Euler deconvolution: Theoretical basis for automatically selecting good solutions, Geophysics, 68, 1962-1968.

Singh, A. and Singh, U. K., 2015, Wavelet analysis of residual gravity anomaly profiles: Modeling of Jharia coal basin, India, 86 (6), 679–686.

Stavrev, P. and Reid, A., 2007, Degrees of homogeneity of potential fields and structural indices of Euler deconvolution, Geophysics, 72, L1-L12.

Stavrev, P. Y., 1997, Euler deconvolution using differential similarity transformations of gravity or magnetic anomalies, Geophysical Prospecting, 45, 207-246.

Thompson, D. T., 1982, EULDPH: A new technique for making computer assisted depth estimates from magnetic data, Geophysics, 47 (1), 31-37.

Verma, R. K., Bhuin, N. C. and Mukhopadhyay, M., 1979, Geology, Structure and tectonics of Jharia Coal Field, India- A 3-D Model, Geoexploration, 17, 305-324.

Verma, R. K. and Ghosh, D., 1974, Gravity survey over Jharia coalfield, India. Geophys. Res. Bull., 12, 165-175.

Verma, R. K., Majumdar, R., Ghosh, Debabrata, Ghosh, Ashish and Gupta, N. C., 1976, Results of Gravity Survey over Raniganj Coalfield, India, Geophysical Prospecting, 24, 19-30.

Verma, R. K., Prasad, S. N. and Jha, B. P., 1973, Magnetic Survey over Jharia Coal Field, Pure and Applied Geophysics, 102 (1), 124-133.

Williams, S., Fairhead, J. D. and Flanagan, G., 2003, Grid based Euler deconvolution: Completing the circle with 2D constrained Euler, SEG Technical Program Expanded Abstracts, 22, 576-579.

Wu, J. S., Jiang, F. and Wang, J. L., 2007, Study of joint inversion of gravity and magnetic data for variable density interface model, Proceeding of Annual of the Chinese Geophysical Society, 633.

Zeyen, H. and J. Pous, 1993, 3-D joint inversion of magnetic and gravimetric data with a priori information, Geophysical Journal International, 112, 244-256.

Zhang, C., Mushayandebvu, M. F., Reid, A. B., Fairhead, J. D. and Odegard, M. E., 2000, Euler deconvolution of gravity tensor gradient data, Geophysics, 65, 512-520.

Zhang, G. B., Shen, N. H., Wang, X. C. and Wang, H. X., 1993, The program system on generalized linear cooperative inversion of the potential anomalies, Journal of Changchun University (Earth Sciences), 23(2), 197-204.